25th ABCM International Congress of Mechanical Engineering
October 20-25, 2019, Uberlândia, MG, Brazil

COB-2019-2387
UNCERTAINTIES ON ADHESIVE LAYER FOR A PLATE STRUCTURE: PASSIVE CONTROL

Guilherme Silva Prado
Heinsten Frederich Leal dos Santos
Universidade Federal de Mato Grosso.
guilhermeprado@ufmt.com
heinsten.leal@gmail.com

Abstract. *Piezoelectric materials have been extensively studied in recent years for the development of harvesting electromechanical devices. The geometric configuration of the piezoelectric patches and the properties adhesive layer rigidity are variables important for the conversion efficiency of mechanical energy to electric energy. This conversion is provided by an electromechanical coupling between a flexible structure and piezoelectric element. So, this work has as objective to present an analysis in passive damping performance of a plate structure in passive control, including a sensibility study in piezoceramic geometric configuration (length and position) and a study on the influence of parametric uncertainties on the thickness properties and Youngs modulus of adhesive bond strength, based on the expected statistical properties of variables, such as expected nominal value, dispersion and positive. All studies presenting in this paper are applied in first vibration mode. For the passive vibration, control performance is evaluated for an located shunted piezoceramic patches. For the study, it was necessary to design resistance and inductance (shunt circuit) of each circuit to see the displacement in two cases: open circuit and closed circuit. This work presents a study on the influence of parametric uncertainties on the thickness properties and Youngs modulus of adhesive bond strength, based on the expected statistical properties of variables, such as expected nominal value, dispersion and positivity.*

Keywords: *Piezoelectric materials, Passive vibration control, Stochastic modeling, Uncertainty analysis, Genetic Algorithms.*

1. INTRODUCTION

Piezoelectric materials have been extensively studied in recent years for the development of control vibrations and harvesting effects. Piezoelectric are materials that have the piezoelectric effect wherever piezoelectric effect is present in two cases: (i) the first is the direct effect wherever to transform mechanical energy in electrical energy; (ii) the second converse effect wherever to transform electrical energy in mechanical displacements. The direct effect has been used for the applications in passive control and harvesting effects, is responsible for the material is the ability to function as a sensor. The converse effect has been used for the application in active control, is responsible for the material is the ability to function as an actuator (Sodano, Inman and Park, 2004).

Several works have been studied ways to optimize control using piezoelectric, changing circuit configurations (Lesieutre 1998; Clark 2000; Reza Moheimani 2003; Viana and Steffen 2006; Lallart et al. 2008), optimizing the distribution of piezoelectric inserts on the host structure (Rosi et al. 2012; Quoc, Tham and Tu, 2018; Shigueoka and Trindade, 2014), using hybrid (passive-active) controls (Trindade) where many use algorithms such as neural networks and genetic algorithms.

The performance of piezoelectric patches for these types of applications is very much dependent on the adequate tuning between resonant, circuit and operation frequencies and on the effective electromechanical coupling between patches and host structure. Therefore, variability and/or uncertainties on material properties, boundary conditions, and bonding effectiveness may have a major effect on reducing the expected or predicted performance of such devices (Santos and Trindade, 2012; Godoy and Trindade, 2012). Still, most of the bonds made between piezoelectric inserts utilize two-part epoxy adhesives (resin and reinforcement), which must be cured at the ideal temperature and pressure to achieve the desired stiffness configuration, so that the curing and mixing process is very likely to be subject to uncertainties (Santos and Trindade, 2016).

This work presents a study on the influence of parametric uncertainties on the thickness properties and *Youngs* modulus of adhesive bond strength (for five piezoelectric localized in positions of the maximums displacements), based on the expected statistical properties of variables, where three functions of parametric distributions (PDF) were adopted, being Gaussian also known as normal, uniform and gamma, such as expected nominal value, dispersion and positive.

2. PROBLEM DESCRIPTION

The structure is composed by a fixed plate of the aluminum with dimension 800 x 500 x 3 mm^3, the piezoelectric (PZT-5H) has dimension 25 x 25 x 0.5 mm^3, as can see in the figure 1. The extension piezoceramics are made of PZT-5H material whose properties are: $\bar{C}_{11}^{D} = 97.767$ GPa, $\rho = 7500 Kg.m^3$, piezoelectric coupling constants $\bar{h}_{31} = 1.3520x10^9$ $N.C^1$, and dielectric constants $\bar{\beta}_{33}^{\varepsilon} = 57.830x10^6 m.F^1$. For the aluminum - mass density $\rho = 2700 Kg.m^{-3}$, $Young's$ modulus $E = 70 GPa$ and Poisson's ratio 0.33. The bonding layer is composed by epoxy glue - mass density $\rho = 1200 Kg.m^{-3}$, $Young's$ modulus $E = 2.5 GPa$ and Poisson's ratio 0.33.(Santos, 2012).

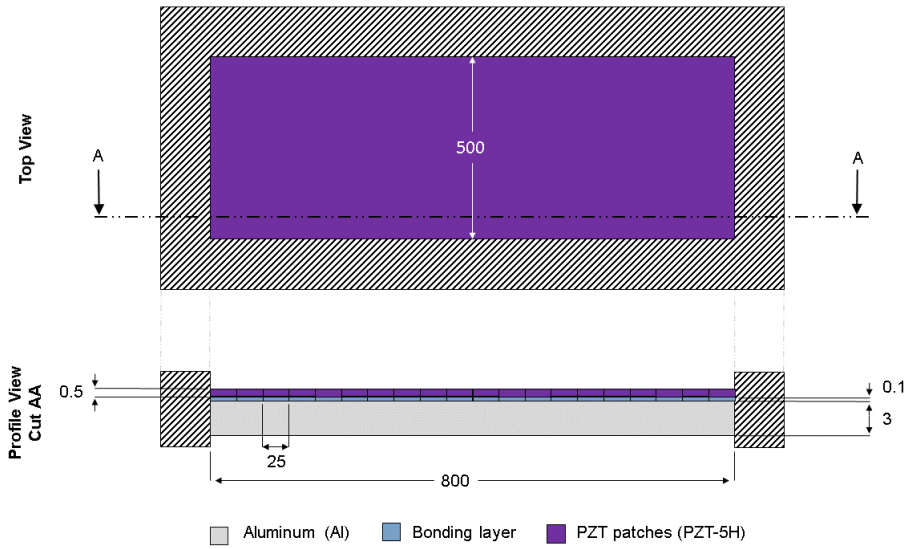

Figure 1. Representation of the plate structure.

Each piezoceramic has a connected Shunt resonant circuit composed of resistance (R) and inductance (L), as can see in figure 2. Thus form is possible to get the mechanical and electrical response for each localization point piezoelectric in structure surface and the maximums displacements points. Tuning the shunt circuit is possible to get the optimal damping by the Joule effect through resistance and to control the frequency by inertia through inductance.

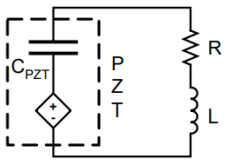

Figure 2. Configuration of the shunt resonant circuit together with the piezoelectric.

3. FINITE ELEMENT MODEL FOR THE STRUCTURE

For the study of the stiffness of the layer was adopted the classic sandwich model (piezoceramic - bonding layer - host), as shown in figure 3. This allows the shear effect that will be responsible for one of the displacement losses of the layers. Thus, Bernoulli-Euler theory is retained for the outer layers, while the bonding layer (Epoxy) is assumed to behave as a Timoshenko beam.

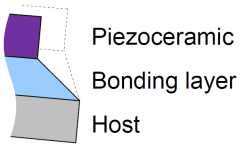

Figure 3. Schematic representation of reduction of transmissibility due to bonding layer.

For the analysis of the output mechanical, the resistance and inductance were optimizations through on genetic algorithm in the function of the tension applied. Were is applied only in the first mode of the vibration.

With the applied theories of the Bernoulli and Timoshenko can be developed the equation of motion for the structure, this form the structure-patches-circuits coupled equations of motion can be written as

$$\begin{bmatrix} \mathbf{M} & 0 \\ 0 & \mathbf{L}_c \end{bmatrix} \begin{Bmatrix} \ddot{\mathbf{u}} \\ \ddot{\mathbf{q}}_p \end{Bmatrix} + \begin{bmatrix} \mathbf{C} & 0 \\ 0 & \mathbf{R}_c \end{bmatrix} \begin{Bmatrix} \dot{\mathbf{u}} \\ \dot{\mathbf{q}}_p \end{Bmatrix} + \begin{bmatrix} \mathbf{K}_m & -\bar{\mathbf{K}}_{me} \\ -\bar{\mathbf{K}}_{me}^t & \bar{\mathbf{K}}_e \end{bmatrix} \begin{Bmatrix} \mathbf{u} \\ \mathbf{q}_p \end{Bmatrix} = \begin{Bmatrix} \mathbf{F} \\ \mathbf{V}_c \end{Bmatrix}, \tag{1}$$

where u and $\mathbf{q}_p$ are the global mechanical displacement and electric charge dofs and $\mathbf{M}$, $\mathbf{K}_m$, $\bar{\mathbf{K}}_{me}$, $\bar{\mathbf{K}}$ are the mass and mechanical, piezoelectric and dielectric stiffness matrices and $\mathbf{F}$ is the mechanical force vector. $\mathbf{L}_c$ and $\mathbf{R}_c$ are diagonal matrices containing the inductance and resistance optimized and $\mathbf{V}_c$ is the vector of electric voltage applied to the electric shunt circuits, but how in this work is studded only the output mechanical the value of the vector of electric voltage is equal zero.

4. VIBRATION CONTROL ANALYSIS

For vibration control analysis, the proposed model (Santos and Trindade 2011) is used to evaluate the mobility (velocity/force) frequency response function of the base structure. The resistive (R) or resonant (RL) shunt circuit affects both the passive and active-passive (hybrid) control performance. In this way, it became necessary to use the circuit that will dissipate the energy or to storage for later use.

4.1 Evaluation of mechanical output under mechanical excitation

How this work analyze a purely mechanical excitation, such as $V_c = 0$ and F = $bfe^{j\omega t}$, the amplitude of a displacement output y = c_yu can be written as $y = G_p\ (\omega) f$, where the FRF $G_p(\omega)$ is

$$\mathbf{G}_p(\omega) = \mathbf{C}_y\omega^2\mathbf{M} + \mathbf{J}\omega\mathbf{C} + \mathbf{K}_m - \mathbf{K}_{me}(\omega^2\mathbf{L}_c + \mathbf{J}\omega\mathbf{R}_c + \mathbf{K}_e)^{-1}\mathbf{K}_{me}\}^{-1} \tag{2}$$

Analyzing the equation 2 it can be noted that the resistance and the inductance have the capacity to change the rigidity properties of the piezoelectric material, in this way it will be applied to the case types i) open-circuit when $\mathbf{R}_c$ tending to infinity and ii) short-circuit when $\mathbf{L}_c = \mathbf{R}_c = 0$. For the open circuit it has

$$\mathbf{G}_p^{oc}\omega = \mathbf{C}_y\{\omega^2\mathbf{M} + \mathbf{J}\omega\mathbf{C} + \mathbf{K}_m\}^{-1}\mathbf{b} \tag{3}$$

To the closed circuit

$$\mathbf{G}_p^{sc}\omega = \mathbf{C}_y\{\omega^2\mathbf{M} + \mathbf{J}\omega\mathbf{C} + \mathbf{K}_m - \mathbf{K}_{me}\mathbf{K}_e\}^{-1}\mathbf{b} \tag{4}$$

You may note that no structural modification is observed in the open circuit box, where as in the case of a short circuit, the rigidity of the piezoelectric patches is reduced.

4.2 Vibration control using piezoelectric actuators and state feedback

This way is necessary to rewrite the motion equations in the form of state space, containing the displacements and modal velocities of the piezoelectric patches and their derivatives of time.

$$\dot{\mathbf{z}} = \hat{\mathbf{A}}\mathbf{z} + \hat{\mathbf{B}}\mathbf{V}_c + \hat{\mathbf{B}}_f\mathbf{f}\ ,\ \mathbf{y} = \hat{\mathbf{C}}_y\mathbf{z}, \tag{5}$$

where

$$\mathbf{z} = \begin{bmatrix} \alpha \\ \mathbf{q}_p \\ \dot{\alpha} \\ \dot{\mathbf{q}}_p \end{bmatrix},\ \hat{\mathbf{A}} = \begin{bmatrix} 0 & 0 & \mathbf{I} & 0 \\ 0 & 0 & 0 & \mathbf{I} \\ -\Omega^2 & \mathbf{K}_p & -\Lambda & 0 \\ \mathbf{L}_c^{-1}\mathbf{K}_p^t & -\Omega_e^2 & 0 & -\Lambda_e \end{bmatrix},\quad \hat{\mathbf{B}} = \begin{bmatrix} 0 \\ 0 \\ 0 \\ \mathbf{L}_c^{-1} \end{bmatrix},\ \hat{\mathbf{B}}_f = \begin{bmatrix} 0 \\ 0 \\ \mathbf{b}_\phi \\ 0 \end{bmatrix},\ \hat{\mathbf{C}}_y = \begin{bmatrix} \mathbf{c}_\phi & 0 & 0 & 0 \end{bmatrix}. \tag{6}$$

The modal displacements are such that $\mathbf{u} = \phi\alpha$ and, for mass normalized vibration modes, $\Omega^2 = \phi^t\mathbf{K}_m\phi$ and $\Lambda = \phi^t\mathbf{C}\phi$. Ω is a diagonal matrix which elements are the undamped natural frequencies of the structure with piezoelectric patches in open-circuit. $\Omega_e^2 = \mathbf{L}_c^{-1}\bar{\mathbf{K}}_e$ and $\Lambda_e = \mathbf{L}_c^{-1}\mathbf{R}_c$ are both diagonal matrices which elements stand, respectively, for the squared natural frequencies of the electric circuits and the ratio between the resistance and inductance. The electromechanical coupling stiffness matrix projected in the undamped modal basis is defined as $\mathbf{K}_p = \phi^t\bar{\mathbf{K}}_{me}$. Input $\mathbf{b}$ and output $\mathbf{c}_y$ distribution vectors are also defined, with modal projections $\mathbf{b}_\phi = \phi^t\mathbf{b}$ and $\mathbf{c}_\phi = \mathbf{c}_y\phi$, and $\mathbf{f}$ is a vector of the amplitudes of each mechanical force applied to the structure (Santos and Trindade 2016).

A linear state feedback for the applied voltages $\mathbf{V}_c$ is assumed such that $\mathbf{V}_c = -\mathbf{gz} = -\mathbf{g}_{dm}\alpha - \mathbf{g}_{de}\mathbf{q}_p - \mathbf{g}_{vm}\dot{\alpha} - \mathbf{g}_{ve}\dot{\mathbf{q}}_p$, where $\mathbf{g}$ is a matrix of control gains for each state variable. Therefore, the state space equation (5) becomes

$$\dot{\mathbf{z}} = (\hat{\mathbf{A}} - \hat{\mathbf{B}}\mathbf{g})\mathbf{z} + \hat{\mathbf{B}}_f\mathbf{f}\ ,\ \mathbf{y} = \hat{\mathbf{C}}_y\mathbf{z}. \tag{7}$$

For a single-input mechanical excitation $\mathbf{f}$, the closed-loop or controlled amplitude of a single displacement output $\mathbf{y}$ can be written such that $\tilde{y} = \mathbf{G}_h(\omega)\tilde{f}$, where the FRF $\mathbf{G}_h(\omega)$ is

$$\mathbf{G}_h(\omega) = \hat{\mathbf{C}}_y(\mathbf{J}\omega\mathbf{I} - \hat{\mathbf{A}} + \hat{\mathbf{B}}\mathbf{g})^{-1}\hat{\mathbf{B}}_f, \tag{8}$$

which can also be derived from the second order equations of motion projected into the undamped modal basis leading to

$$\mathbf{G}_h(\omega) = \mathbf{c}_\phi\left\{-\omega^2\mathbf{I} + \mathbf{J}\omega(\Lambda + \mathbf{K}_p\mathbf{D}_{cc}^{-1}\mathbf{g}_{vm}) + [\Omega^2 + \mathbf{K}_p\mathbf{D}_{cc}^{-1}(\mathbf{g}_{dm} - \mathbf{K}_p^t)]\right\}^{-1}\mathbf{b}_\phi, \tag{9}$$

where the closed-loop dynamic stiffness of the electric circuit $\mathbf{D}_{cc}$ is

$$\mathbf{D}_{cc} = -\omega^2\mathbf{L}_c + \mathbf{J}\omega(\mathbf{R}_c + \mathbf{g}_{ve}) + (\bar{\mathbf{K}}_e + \mathbf{g}_{de}). \tag{10}$$

In this work, the control gain $\mathbf{g}$ is calculated using the standard optimal LQR control theory applied to a single-input/single-output case, that is with only one active-passive patch-circuit pair for the control to minimize the vibration amplitude at one specific location of the structure, such that the following objective function is minimized

$$J = \frac{1}{2}\int_0^\infty \left(\dot{y}^2 + rV_c^2\right)dt, \tag{11}$$

where $\dot{y}$ is the velocity at one location of interest and V_c is the control voltage applied to the active-passive shunt circuit in all cases following an iterative routine proposed in (Trindade, Benjeddou and Ohayon, 1999).

5. STOCHASTIC MODELING FOR UNCERTAINTY QUANTIFICATION

Became an approach for analyzing random uncertainties for the bonding stiffness main parameter, that is the effective *Young′s* modulus E_b of the adhesive. This is done considering the *Young′s* modulus as a stochastic variable, respecting a given probability density function. Random realizations of the stochastic variable E_b are then generated.

An appropriate probabilistic model for the stochastic variable is constructed accounting for the available information only, which is the following: (i) the support of the probability density function is $]0,+\infty[$; (ii) the mean values are such that $E[X] = X$; and (iii) zero is a repulsive value for the positive-valued random variables which is accounted for by the condition $E[ln(X)] = cX$ with $jcX < +\infty$. Therefore, the Maximum Entropy Principle yields the following Gamma probability density functions for X (Soize, 2001; Cataldo et al., 2009; Ritto et al., 2010).

The probability density function for the adhesive *Young′s* modulus is not known. Moreover, it is not possible to characterize its probability density function through of the measure physical, since the bonding stiffness depends not only on a manual mixture of two components (resin and hardener) but also on of the others effects as temperature and pressure. Therefore, the effective bonding stiffness would have to be characterized after assembling.

Nevertheless, it is expected that a mean (or nominal) value could be estimated and, also, that it should be positive so a reasonable stochastic model can be constructed from a Gamma probability density function (PDF), present in equation 12.

$$P_E(E) = \mathbb{I}_{]0,+\infty[}\left(\frac{1}{\delta_E^2\bar{E}}\right)^{\delta_E^{-2}}\frac{E^{\delta_E^{-2}-1}}{\Gamma(\delta_E^{-2})}\exp\left(-\frac{E}{\delta_E^2\bar{E}}\right), \tag{12}$$

in which $\delta_E = \sigma_E/\bar{E}$ is the relative dispersion of stochastic bonding layer *Young′s* modulus E_b and σ_E is its standard deviation. The Gamma function is defined as $\Gamma(x) = \int_0^\infty t^{x-1}e^{-t}dt$.

For comparative study, is necessary the use other density function distribution possessing mean of value upward of $2.5Gpa$. In this way probability density function considered for the adhesive *Youngs* modulus is the Truncated Gaussian PDF. The Gaussian PDF, also known as Normal PDF, is given by

$$P_E(E) = \mathbb{I}_{]-\infty,+\infty[}(E)\frac{1}{\sigma_E\sqrt{2\pi}}e^{-\frac{(E-\bar{E})^2}{2\sigma_E^2}}. \tag{13}$$

Notice that the support of the Gaussian PDF is $]-\infty,+\infty[$ and, thus, it may lead to negative values for the adhesive $Young's$ modulus. Therefore, is be necessary to truncate the PDF in order to admit only positive values, considering $\bar{E} = 2.5GPa$, $\delta_E = 94\%$, until all are within the range of acceptable.

Other density function distribution used if Uniform PDF possessing mean of value upward of $2.5Gpa$ defined by $E(X) = \frac{1}{2}(a+b)$. In this way probability density function considered for the adhesive $Young's$ modulus defined by minimums and maximums parameters $[a,b]$ defined by $]0,+\infty[$ for present work. The Uniform PDF is given by

$$P_E(X \in [x, x+d]) = \int_x^{x+d} \frac{dy}{b-a}. \tag{14}$$

The figure 4 show tree histograms of the simple generated with these parameters.

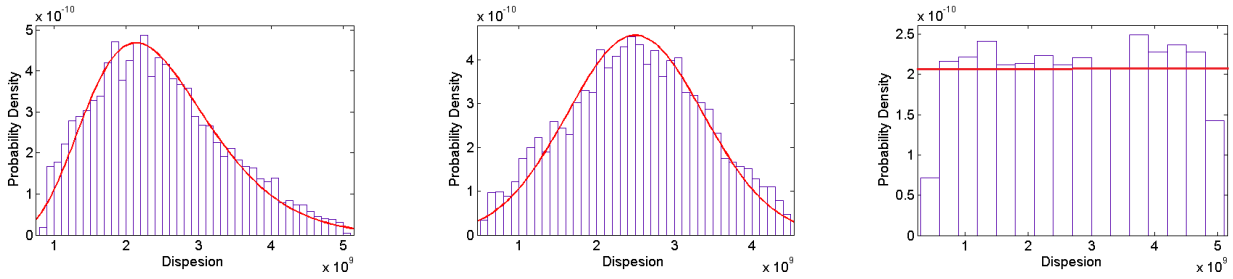

Figure 4. Gamma probability density function, Normal probability density function and Uniform probability density function of simple using 5000 realizations.

The statistical analyses of the FRF amplitudes were performed using their 5000 realizations at each frequency to calculate the corresponding mean values and 95% confidence intervals. The 95% confidence intervals were evaluated using the 2.5% and 97.5% percentiles of the realizations of FRF amplitudes at each frequency. Figure 5 summarizes the simulation procedure.

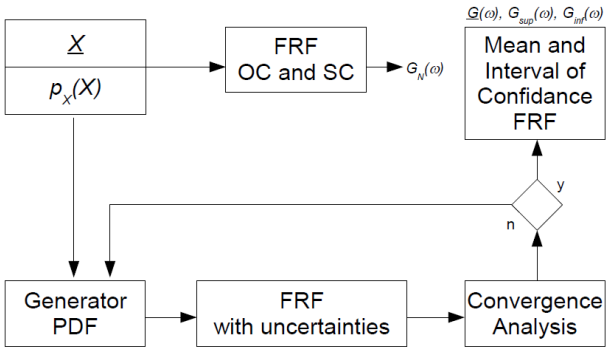

Figure 5. Schematic representation of the computational procedure to obtain the confidence intervals for the frequency response functions $G_p(\omega)$ and $G_h(\omega)$

.

6. GENETIC ALGORITHM METHOD

The Genetic Algorithm (GA) can be described as a family of computational models that are inspired by the evolution of species for problem solving. They incorporate potential solutions to a problem in species of chromosomes, or population,that pass through segregation and data crossing, applying a selection nature that seeks to filter the results that best match the solution of the problem, selecting them positively for future crossings and penalizing those that flee the possible solution of the problem, thus forcing the structure to converge to a single value that meets the nature of the formulation.

In present work a genetic algorithm was used to get the best resistance and inductance values of the shunt resonant circuit. The figure 6 shows these both techniques were using aiming to optimize the parameters of resistance and inductance of the associated circuit.

7. RESULTS

For the first structure configuration, can see in figure 1, realized a analyze of mechanical and electrical response, and the best piezoceramic positions.

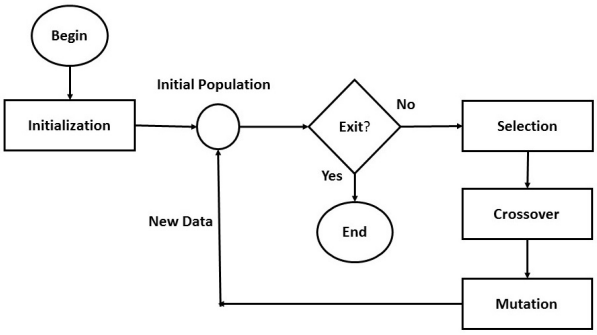

Figure 6. Algorithm Genetic Flowchart

7.1 Selection the best piezoceramic positions

The first vibration mode are shown in figure 7 for piezoelectric positioned in all surface of the plate. The first vibration mode frequency is 37.75Hz. Note that, as piezoelectric has its direct effect proportional to the applied strain / strain, it is expected that the best positions will be at the highest displacement points, at the largest points of strain (in the regions of greatest curvature).

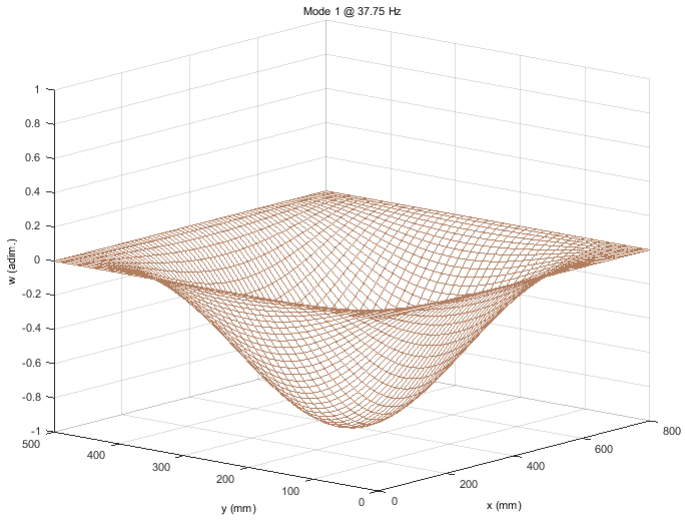

Figure 7. First vibration mode for the plate with piezoelectric patches located at the all plate surface.

The plate has piezoceramics fixed in all surface where each piezoceramic is connected in a Shunt Circuit. This form, it is possible to see the points of maximums deformations for a open circuit configuration and to analyze the bests piezoceramic localization for the harvesting effects or passive vibration control, as we can see in figure 8.

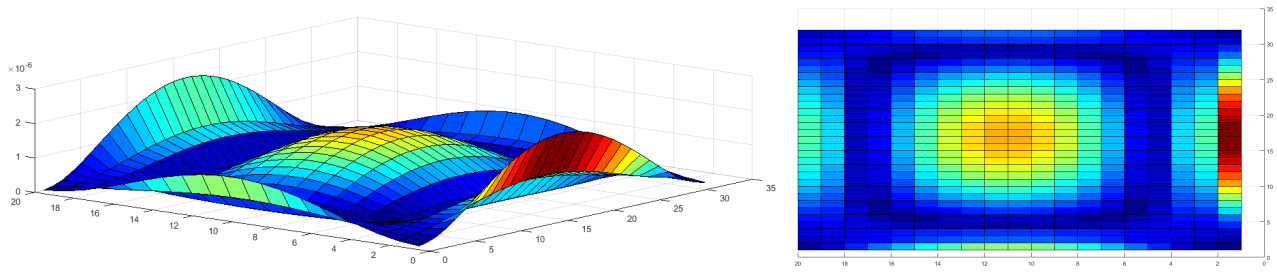

Figure 8. Mechanical response for the first mode vibration in laminate plate with piezoceramic patches located by all surface of the structure.

Based in mechanical response present in figure 7 and in deformation present in figure 8 were positioned piezoelectric

at the five largest displacements points. The localization representation of the piezoelectrics can be see in figure 9.

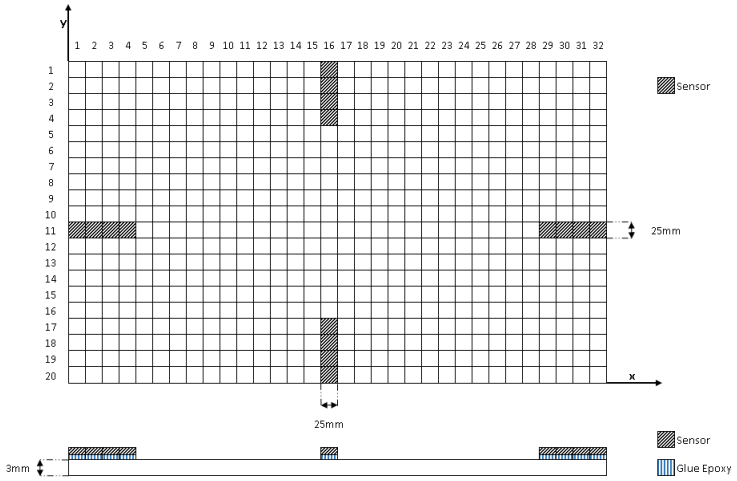

Figure 9. Piezoelectric positioning.

The response frequency of the structure show in figure 9 can be see in figure 10. The positioning of sixteen piezoelectric is based on minimizing a range of motion.

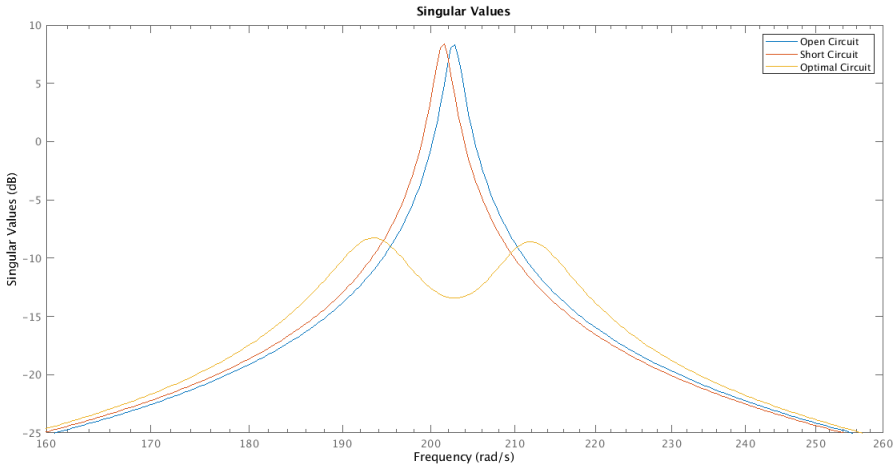

Figure 10. Frequency response function of the laminate plate for the first vibration mode.

7.2 Uncertainty Quantification Results

For analyzing random uncertainties Monte Carlo simulation were performed and the realizations of the frequency response functions, were used to evaluate their mean values and 95% confidence intervals, using 2.5% and 97.5% percentiles of the realizations. The effect of uncertainties about the efficiency were analyzed in function of the frequency response, where this case were applied only for the first mode of vibration. This where applied in the tree distributions proposed.

7.2.1 Normal Probability Density Function

For this configuration, the mean and 95 % confidence interval for the frequency response of the shunted plate subjected to uncertainties of bonding layer stiffness compared to the short-circuit condition (without passive control). The interval of confidence presented an alteration on the resonance, making the peak of resonance displaced to the left, this represent more values lower 2.5 GPa in the Normal probability density function.

May notice that the nominal model indicates a passive reduction in the vibration amplitude of 7.8 dB (considering the difference between peak responses for SC and RL), while when considering the uncertainties is found to be in the range 0.3 dB for superior or -16 dB for inferior bound.

7.2.2 Gamma Probability Density Function

For this configuration shows the mean and 95 % confidence interval for the frequency response of the shunted cantilever beam subjected to uncertainties of bonding layer stiffness compared to the short-circuit condition (without passive control).The interval of confidence presented an alteration on the resonance, making the peak of resonance displaced to the left, this represent more values lower 2.5 GPa in the Gamma probability density function.

May notice that the nominal model indicates a passive reduction in the vibration amplitude of 7.8 dB (considering the difference between peak responses for SC and RL), while when considering the uncertainties is found to be in the range 1.3 dB for superior or -17.4 dB for inferior bound.

7.2.3 Uniform Probability Density Function

For this configuration shows the mean and 95 % confidence interval for the frequency response of the shunted cantilever beam subjected to uncertainties of bonding layer stiffness compared to the short-circuit condition (without passive control).The interval of confidence presented an alteration on the resonance, making the peak of resonance displaced to the right, this represent more values lower 2.5 GPa in the Gamma probability density function.

May notice that the nominal model indicates a passive reduction in the vibration amplitude of 7.8 dB, while when considering the uncertainties is found to be in the range 0.4 dB for superior or -16 dB for inferior bound.

8. CONCLUSION

An analysis of the effect of uncertainties of the bounding layer stiffness on the piezoelectric vibration control was performed. In passive (shunted) vibration control, bonding stiffness uncertainties mainly affect the tuning between electric circuit and piezo-structure, reducing the overall performance. Future works can be performed for new results using uncertainties on Poisson ratio and thickness of the layers.

9. REFERENCES

Akhras, G., 2000, "Smart Materials and Smart Systems for the Future", Canadian Military Journal, Vol.1 *N*3, pp.24-31.

Benjeddou, A. e Ranger, J.A., 2006. *Use of shunted shear-mode piezoceramics for structural vibration passive damping.* Computers and Structures. Vol 84, pp.1415-1425.

Clark, R. L., Saunders, W. R. e Gibbs, G. P., 1998, "Adaptive Structures − Dynamics & Control", John Wiley & Sons, Inc.

Den Hartog, J. P., 1956, *Mechanical Vibrations*, Fourth Edition, McGraw-Hill.

Godoy, T. C. de; Trindade, M. A.; Deu, J.-F.; " Topological optimization of piezoceramic energy harvesting devices for improved eletromechanical efficiency and frequency range", p. 4003-4016 . In: In Proceedings of the 10th World Congress on Computational Mechanics [Blucher Mechanical Engineering Proceedings, v. 1, n. 1]. São Paulo: Blucher, 2014. ISSN 2358-0828, DOI 10.5151/meceng-wccm2012-19664

Hagood, N. W. e von Flotow, A., 1991, *Damping of Structural Vibrations with Piezoelectric Materials and Passive Electrical Networks*, Journal of Sound and Vibration, Vol. 146, N2, pp.243-268.

Lesieutre, G. A., 1998, *Vibration Damping and Control using Shunted Piezoelectric Materials*, Shock and Vibration Digest, Vol. 30, pp 181-190.

Lesieutre, G. A.; LEE, U. A finite element for beams having segmented active constrained layers with frequency-dependent viscoelastic. Smart Mat. Struct.5, USA, p. 615âĂŞ627, 1996.

S.O. Reza Moheimani. A survey of recent innovations in vibration damping and control using shunted piezoelectric transducers. IEEE Transactions on Control Systems Technology, 11(4):482âĂŞ494, 2003.

Santos, H.F.L., and Trindade, M.A. Modeling of a sandwich beam with thickness-shear active-passive piezoelectric networks. In 19th ABCM International Congress of Mechanical Engineering (COBEM 2007), Brasilia, 2007. Proceeding of the 19th International Congress of Mechanical Engineering., 2007.

Santos, H. F. L., *Controle de vibrações estruturais usando cerâmicas piezoeletricas em extensão e cisalhamento conectadas a circuitos hibridos ativo-passivos*. 2008. 109p. Dissertação (Mestrado em Egenharia Mecânica) - Escola de Engenharia de São Carlos da Universidade de São Paulo, São Carlos, 2008.

Shigueoka, A.H. ; TRINDADE, M.A.. Continuous optimization of discrete modal filters applied to flexible structures. Em: Congresso Nacional de Engenharia MecÃćnica (CONEM 2014), 2014.

Sodano H.A., Inman D.J. and Park G., A review of power harvesting from vibration using piezoelectric materials. Shock and Vibration Digest. 36(3):197-206, 2004.

Trindade M.A. and Maio C.E.B., Multimodal passive vibration control of sandwich beams with shunted shear piezoelectric materials. Smart Materials and Structures. 17:055015, 2008.

Trindade, M. A., Benjeddou, A. e Ohayon, R., 2001. *Piezoeletric active vibration control of damped sandwich beams*.

Journal of Sound and Vibration. Vol 246, N 4. pp.653-677.

Trindade, M. A., et al. Structural vibration control using piezoelectric materials. In Brazil AFOSR Workshop on Advanced Structural Mechanics and Computational Mathematics, Campinas, 2008. Brazil AFOSR Workshop on Advanced Structural Mechanics and Computational Mathematics. : UNICAMP/AFOSR, 2008.

Viana, F. A. C., *Amortecimento de vibrações utilizando pastilhas piezeletricas e circuitos* shunt *ressonantes*. 2005. 132p. Dissertação (Mestrado em Engenharia Mecânica) - Universidade Federal de Uberlândia, Uberlândia, 2005.

10. RESPONSIBILITY NOTICE

The authors are the only responsible for the printed material included in this paper.